DIAmante space-based photometry of the PLATO South Field (LOPS2)

Marco Montalto
INAF – Osservatorio Astrofisico di Catania

Abstract

The first long pointing field of PLATO has been recently selected (LOPS2[1]). Accurate characterization of this region of the sky is of great relevance for the preparation and future success of PLATO. It is possible to derive space-based photometry of stars in LOPS2 before the launch of PLATO given that the TESS (Ricker et al. 2015) satellite has repeatedly observed it during the past years.

The DIAmante pipeline is based on the difference imaging approach and has already provided accurate photometry of PLATO targets in the past. When coupled with traditional and innovative transit search techniques it has permitted the identification of hundreds of new transiting candidates (Montalto et al. 2020, 2023; Melton et al. 2023, Melton et al. 2024a,b).

Here I present the preparation of a novel set of DIAmante photometric measurements focused on LOPS2. The stars in the field have been selected form Gaia DR3 (Gaia Collaboration et al. 2023) and include both PLATO targets and contaminant sources down to a preselected PLATO magnitude limit. This set is broader than the one in the target PLATO Input Catalog (tPIC; Montalto et al. 2021) both in terms of magnitude limit and in terms of spectral type coverage. The analysis of these light curves with different algorithms will be crucial for the characterization of PLATO targets and their contaminants, for the identification additional targets of scientific interest for PLATO and for the future interpretation of PLATO results.

1 - https://platomission.com/2023/07/11/first-plato-long-duration-observation-phase-lop-field-selected/

1. The DIAmante pipeline

Several approaches have been presented for the analysis of TESS Full Frame Images (FFIs, e.g. Oelkers & Stassun 2018, AJ, 156, 132; Bouma et al. 2019, ApJS, 245, 13 ; Feinstein et al. 2019, PASP, 131, 094502; Nardiello et al. 2019, MNRAS, 490, 3806; Nardiello et al. 2020, MNRAS, 495, 4924). In this project, I employed a method described in Montalto et al. (2020) based on the differential imaging analysis (DIA; Alard & Lupton 1998, ApJ, 503, 325; Alard 2000, A&AS, 144, 363; Bramich 2008, MNRAS, 386, L77; Miller, Pennypacker & White 2008, PASP, 120, 449). Difference imaging permits a very efficient subtraction of all constant sources in the field, reduces the impact of contaminants on the target's photometry and permits a more accurate estimate of the sky background with respect to simple aperture photometry (Fig. 1).

First iteration

$$\mathrm{R} \otimes \mathrm{K} + \mathrm{B} = \mathrm{I}$$

$$\mathrm{K_{p,q}(i,j)} = \begin{cases} 1 \text{ if } (\mathrm{i} = \mathrm{p} \wedge \mathrm{j} = \mathrm{q}) \\ 0 \text{ if } (\mathrm{i} \neq \mathrm{p} \vee \mathrm{j} \neq \mathrm{q}) \end{cases}$$

Constant δ-function basis kernel

Second iteration

The background term (B) is substituted with a differential background model (B_{im}) constructed from a filtered and smoothed version of the first iteration residual image, which is then simultaneously fit together with the kernel

$$\mathrm{R} \otimes \mathrm{K} + \mathrm{B'} = \mathrm{I}$$

$$\mathrm{B'} = \mathrm{B_1} \times \mathrm{B_{im}} + \mathrm{B_2}$$

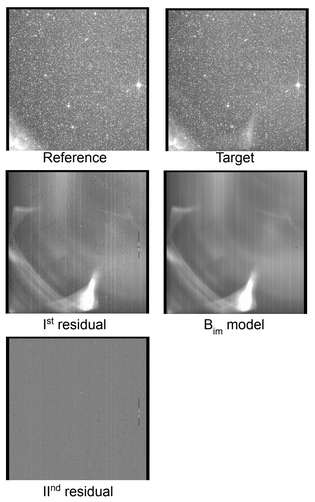

Fig. 1 - From the top left: reference image,target image, first residual image, differential background (B_{im}) model and final, second residual image.

2. Selection of the sample

2.1 - The sample

The sample was constructed selecting all sources within a radius of 28.5 degrees from the center of the LOPS2 field in the Gaia DR3 catalog (94 725 017 stars). Then, all sources with PLATO magnitude P<16 (see Sect. 2.2), distance not null from Bailer-Jones et al. (2021) and for which it was possible to determine reddening and extinction were selected (5 811 247 stars).

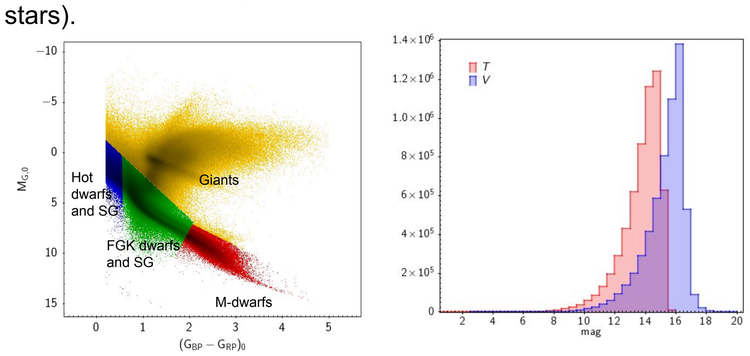

Fig. 2 - *Left:* absolute, intrinsic color-magnitude diagram of the selected stars with different stellar populations highlighted by different colors. *Right:* histogram of the apparent magnitudes of the selected stars in the TESS *T*-band (red) and in the visible *V*-band (blue).

Figure 2 (left) shows the absolute, intrinsic color-magnitude diagram of the selected stars and figure 2 (right) shows the corresponding apparent magnitudes in terms of the TESS *T*-band (red histogram) and the visible *V*-band (blue histogram).

2.2 - Calculation of the PLATO magnitude

Library	Temperature range	R	# models dwarfs	# models giants
MPSA	3500 K - 9000 K	55	56	56
MARCS	2500 K - 8000 K	20000	31	31
POLLUX/AMBRA	3500 K - 8000 K	>150000	18	17
POLLUX/BT-Dusty	2100 K - 6000 K	>100000	39	41
POLLUX/CMFGEN	12020 K - 63880 K	150000	35	35
COELHO	3500 K - 7000 K	275000	15	15

Tab. 1 - This table shows the temperature range, the spectral resolution (R) and the number of synthetic spectra of each stellar library used for the calculation of the PLATO magnitude.

The calculation of the PLATO magnitude was done using synthetic spectra from different stellar libraries. The libraries include spectra with different temperatures and spectral resolution as shown in Table 1.

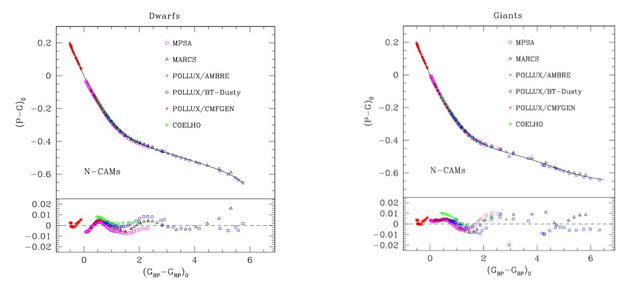

Fig. 3 - Calibration relations between Gaia DR3 magnitudes and PLATO magnitude for normal cameras (N-CAMs) and for dwarfs (left) and giants (right) stars. The bottom panels show the residuals between synthetic colors and best-fit interpolation polynomials.

The PLATO magnitude was defined in the VEGA system. A calibration relationship was calculated (both for dwarfs and for giants) between the PLATO and the Gaia DR3 synthetic magnitudes in the form $(P\text{-}G)_0$ vs $(G_{BP}\text{-}G_{RP})_0$ as illustrated in Fig. 3. The resulting calibration relationships can be found in PLATO-SCI-UP-TN-0019.

References

Alard & Lupton 1998, ApJ, 503, 325; Alard 2000, A&AS, 144, 363; Bailer-Jones et al. 2021, AJ, 161, 147; Bouma et al. 2019, ApJS, 245, 13; Bramich 2008, MNRAS, 386, L77; Feinstein et al. 2019, PASP, 131, 094502; Gaia Collaboration et al. 2023, A&A, 674, 22; Miller, Pennypacker & White 2008, PASP, 120, 449; Melton et al. 2023, arXiv230206744; Melton et al. 2024a, AJ, 167, 202; Melton et al. 2024b, AJ, 167, 203; Montalto et al. 2020, MNRAS, 498, 1726; Montalto et al. 2021, A&A, 653, 98; Montalto et al. 2023, MNRAS, 518, 31; Nardiello et al. 2019, MNRAS, 490, 3806; Nardiello et al. 2020, MNRAS, 495, 4924; Ricker et al. 2015, JATIS, 1, 014003; Oelkers & Stassun 2018, AJ, 156, 132; Kunimoto et al. 2022, AJ, 163, 290

3. TESS observations of the LOPS2 field

3.1 - TESS coverage of the LOPS2 field

The targets selected across the LOPS2 field have been observed during multiple sectors by TESS. Figure 4 shows for how many sectors the targets in LOPS2 have been observed by TESS including both nominal and extended mission data (Sectors 1 - 67).

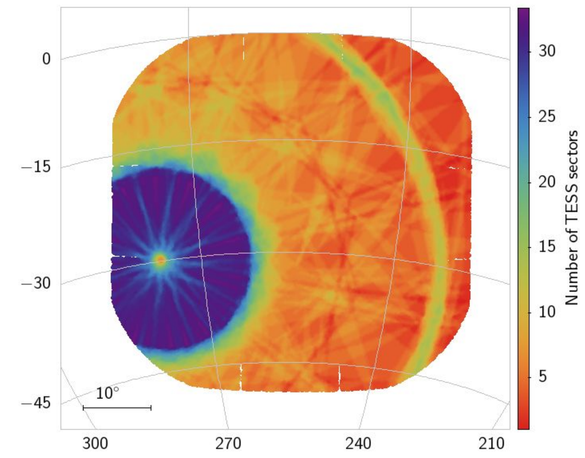

Fig. 4 - Number of TESS sectors for targets across the LOPS2 field.

3.2 - Photometric precision of PLATO vs TESS

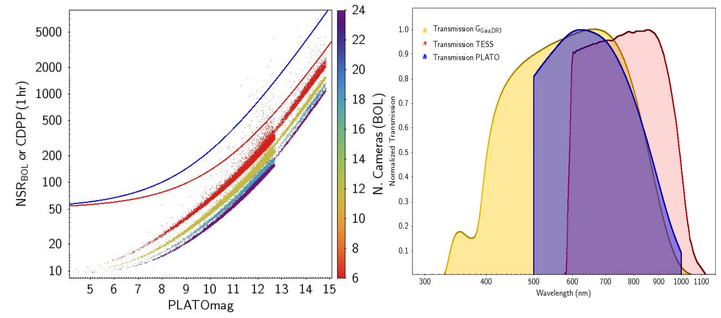

Fig. 5 - In the left panel it is shown the photometric precision of PLATO (colored points) and TESS (colored curves) as a function of the PLATO magnitude. The blue curve is indicative of the TESS photometric precision for F-type dwarf stars, the red curve for M-type dwarf stars. In the right panel the bandpasses of Gaia DR3 (*G*-band, yellow), PLATO (normal cameras, blue) amd TESS (red) are shown.

Figure 5 (left panel) reports the Noise-to-Signal ratio at Beginning Of Life for PLATO tPIC2.0 targets in LOPS2 (NSR_{BOL} colored points) and the Median CDPP in 1hr for all 230 000, 2-minute targets processed by the TESS Science Processing Operations Center (SPOC) pipeline across the Primary Mission (Kunimoto et al. 2022, red and blue curves), as a function of the PLATO magnitude. The blue curve is indicative of the TESS photometric precision for F-type dwarf stars, the red curve for M-type dwarf stars, while the colored points represent the number of PLATO cameras that will observe each target as indicated by the color scale on the right side. In the right panel of Figure 5, the normalized transmission curves of Gaia DR3 (*G*-band, yellow), PLATO (normal cameras, blue) and TESS (red) are shown.

Conclusions

A set of 5 811 247 stars in the LOPS2 field has been selected on the basis of their calculated PLATO magnitudes and it is analyzed with the DIAmante pipeline to produce the light curves of PLATO stars observed by TESS. These light curves can be analyzed with different algorithms to characterize PLATO targets and their contaminants, to identify additional targets of scientific interest for PLATO and to permit the future interpretation of PLATO results.